

The Effect of Hydrogen Bonding on Polymerization Behavior of Monofunctional Vinyl Cyclopropane-Amides with Different Side Chains

Sören Schumacher, Sanwardhini Pantawane, Stephan Gekle, and Seema Agarwal*

The synthesis of four different monofunctional vinyl cyclopropane (VCP) amides and their photopolymerization behavior are presented. All VCPs can form hydrogen bonds, with one being the amide linkage of the VCP unit and the other one being the side chain. The number of additional hydrogen bonds is regulated by the different side chains being, carbonate, urethane, urea, and amide. Hydrogen bonds should lead to a preorganization of the monomers, leading to a fast polymerization. Kinetic studies of the photopolymerization, analysis of hydrogen bond strength via solid-state nuclear magnetic resonance (NMR) experiments, and theoretical calculations are used to correlate the degree of conversion and the amount of preorganization. A fast polymerization could be observed due to hydrogen bonding near the active site, while hydrogen bonds in the side chain make a minor difference.

lowest shrinkage was observed.^[4,6] Such monomers are of interest as photopolymerizable systems, for example, for precise coatings,^[7] dental fillings,^[8] and microlithography.^[9] One disadvantage of the well-studied VCP-ester derivatives is the slow and incomplete polymerization.^[6,10] In previous work, we introduced a new class of amide-linked bifunctional VCP (bis-VCP-amide), which showed a much faster and complete polymerization.^[11] In VCP-amides, the spacer is attached to the cyclopropane ring via an amide linkage. This linkage led to a preorganization in a chain-like arrangement of the monomers via hydrogen bonding and, therefore, fast polymerization. Since then, several new VCPs have been introduced, following


the same concept.^[5,12] While bifunctional systems are needed for getting a cross-linked thermoset for real applications, the concept of preorganization cannot be investigated systematically in these systems. The cross-linking introduces insolubility making structural characterization and kinetic studies difficult. Therefore, in a recent study, we investigated the role of hydrogen-bond (H-bond) sites by introducing different organic functional groups in the side chain of monofunctional VCPs, keeping the linker between the side chain and VCP as ester on polymerization behavior. Although H-bonding influenced the rate of polymerization, the difference among the different functional groups was little, as the hydrogen bonding site was too far from the active site.^[13] This finding agrees with a previous report, where the rate of polymerization could be correlated to the distance between hydrogen bond and active site for acrylate monomers.^[14] Therefore, we now present a new set of monomers, which bear H-bonding sites at two different positions in VCPs: an amide group linking the sidechain to the cyclopropane ring and different organic functional groups (amide, urethane, and urea) capable of H-bonding to different extents in the side chain to compare their behavior in free-radical photopolymerization concerning the rate of polymerization, and monomer conversion. For comparison, a non-hydrogen-bonding side chain (carbonate functional group) VCP-amide was also prepared. The aim is to obtain a full picture on how both the H-bonding sites affect the polymerization behavior of monofunctional VCPs. In addition, we compare the experimental findings with the theoretical calculations, which might enable a better and faster prediction of structural designs of mono- or bifunctional systems in the future.

1. Introduction

Vinyl cyclopropanes (VCPs) have found various interests in organic chemistry, where they act as starting materials for complex structures^[1] and polymer science.^[2] They were introduced as radically polymerizable monomers, showing low volume shrinkage during polymerization.^[3–5] This is due to the radical ring-opening mechanism, whereby additional bonds are introduced into the backbone, compensating for the shrinkage of the formation of covalent bonds. While both thermal and photopolymerization of such systems were investigated, light-induced polymers'

S. Schumacher, S. Agarwal
 Macromolecular Chemistry II
 University of Bayreuth
 Universitätsstraße 30, 95440 Bayreuth, Germany
 E-mail: agarwal@uni-bayreuth.de

S. Pantawane, S. Gekle
 Biofluid Simulation and Modeling
 Theoretische Physik VI
 Universität Bayreuth
 Universitätsstraße 30, 95440 Bayreuth, Germany

 The ORCID identification number(s) for the author(s) of this article can be found under <https://doi.org/10.1002/macp.202200155>

© 2022 The Authors. Macromolecular Chemistry and Physics published by Wiley-VCH GmbH. This is an open access article under the terms of the Creative Commons Attribution License, which permits use, distribution and reproduction in any medium, provided the original work is properly cited.

DOI: 10.1002/macp.202200155

2. Experimental Section

2.1. Materials

1,4-Dibromo-2-butene, diethyl malonate, sodium, *tert*-butyl dicarbonate, and camphorquinone (CQ) were supplied by Aldrich and used without further purification. 4-(dimethylamino) pyridine (DMAP) and ethyl 4-dimethylaminobenzoate (EDMAB) (Fluka) were used without further purification. Ethyl isocyanate, ethyl chloroformate, *N*-Boc-ethanolamine, *N*, *N'*-dicyclohexylcarbodiimide (DCC), and ethylenediamine were supplied by Alfa Aesar and used without further purification. Potassium hydroxide (Carl Roth), magnesium sulfate, and triethylamine (Güssing) were used without further purification. Sodium bicarbonate (Fisher chemical) was used without further purification. Sulfuric acid and ammonium chloride were supplied by VWR and used without further purification. All solvents were distilled before use.

2.2. Analytical Methods

¹H- (300 MHz) and ¹³C-nuclear magnetic resonance (NMR) spectra (75 MHz) were recorded on a Bruker Ultrashield-300 spectrometer at room temperature. To distinguish between primary and tertiary or secondary and quaternary carbons, ¹³C Attached Proton Test (APT) was conducted. The 2-dimensional (2D) NMR heteronuclear single quantum coherence (HSQC) experiments were performed to observe $1 J$ coupling and Heteronuclear Multiple Bond Correlation (HMBC) experiments for coupling $J > 1$. Solid-state NMR (2.0 kHz) was recorded on a Bruker Advance III HD NMR 400 (field strength 9.4 T) with a 3.2 mm sample carrier. Variable ¹H temperature experiments have been performed from 25 to 60 °C. Differential scanning calorimetric (DSC) measurements were performed on a NETZSCH DSC 204 F1 Phoenix under a nitrogen atmosphere with 20 mL per min flow. Thermogravimetric analysis was performed in alumina pans with sample masses of around 5 mg and a flow rate of 50 mL per min on a NETZSCH Libra F1 device.

2.3. Monomer Synthesis

The VCP derivatives 1-(2-((ethoxycarbonyl)oxy)ethyl) 1-ethyl 2-vinyl cyclopropane-1,1-dicarboxylate [Monomer 1], 1-ethyl 1-(2-propionamidoethyl) 2-vinyl cyclopropane-1,1-dicarboxylate [Monomer 2], 1-ethyl 1-(2-(3-ethylureido)ethyl) 2-vinyl cyclopropane-1,1-dicarboxylate [Monomer 3] and 1-(2-((ethoxycarbonyl)amino)ethyl) 1-ethyl 2-vinyl cyclopropane-1,1-dicarboxylate [Monomer 4] were synthesized in three steps. The first two steps were the typical reaction sequences for the synthesis of VCP derivatives. Diethyl 2-vinyl cyclopropane-1,1-dicarboxylate and the hydrolyzed diethyl 2-vinyl cyclopropane-1,1-dicarboxylate in the first two steps were synthesized as per the published procedure.^[4,15] The last step was the amidation of hydrolyzed diethyl 2-vinyl cyclopropane-1,1-dicarboxylate with corresponding amines; 2-aminoethyl ethyl carbonate (5), ethyl (2-aminoethyl)carbamate (6), 1-(2-aminoethyl)-3-ethyl urea (7),

N-(2-aminoethyl)propionamide (8). The synthesis of amines 5, 6, 7, and 8 are given in the Supporting Information (For reaction schemes and corresponding NMR spectra, see Figures S1–S7, Supporting Information).^[16]

2.4. General Procedure for Preparation of VCP Ester Derivates

Under argon 1-(ethoxycarbonyl)-2-vinyl cyclopropane-carboxylic acid (1.1 equiv.), 6-chloro-1-hydroxy benzotriazole (HOBt-Cl) (1.15 equiv.), and the corresponding amine (1.0 equiv.) were dissolved in dry dichloromethane (DCM). At 0 °C, triethylamine (NEt₃) (2.2 equiv.) was added, and the reaction mixture was stirred for 15 min. At 0 °C in dry DCM, dissolved DCC (1.1 equiv.) was slowly added. The reaction mixture was stirred at 0 °C for 1 h and at room temperature for 17 h. The reaction mixture was filtered, and the filtrate was washed three times with 0.5 M hydrochloric acid (HCl), saturated sodium bicarbonate (NaHCO₃), and saturated sodium chloride (NaCl) solution, respectively. The organic phase was dried over magnesium sulfate (MgSO₄), and the solvent was removed under reduced pressure. The product was obtained after purification using flash chromatography.

2.4.1. 1-(2-((ethoxycarbonyl)oxy)ethyl) 1-ethyl 2-vinyl cyclopropane-1,1-dicarboxylate [Monomer 1]

4.17 g of 1-(ethoxycarbonyl)-2-vinyl cyclopropane-carboxylic acid (22.6 mmol) was reacted with 4.05 g HOBt-Cl (23.9 mmol), 4.0 g NEt₃ (5.5 mL, 39.7 mmol), 2.51 g 2-aminoethyl ethyl carbonate (18.9 mmol), and 4.09 g DCC (23.9 mmol). DCC was dissolved in 50 mL DCM, added into the reaction mixture, dissolved in 30 mL DCM. Flash chromatography was used for purification (cyclohexane: EtOAc 9:1 → 7:3). White solid, yield: 66%. NMR and FTIR experiments were conducted for structural verification (see Figures 1–3 and Figures S8–S11, Supporting Information).

¹H NMR (300 MHz, CDCl₃) δ 8.66 (s, 1H), 5.71–5.57 (m, 1H), 5.33 (dd, $J = 17.1, 1.5$ Hz, 1H), 5.16 (dd, $J = 10.2, 1.5$ Hz, 1H), 4.28–4.13 (m, 6H), 3.64–3.54 (m, 2H), 2.53 (dd, $J = 17.1, 8.7$ Hz, 1H), 2.08–1.99 (m, 1H), 1.91–1.83 (m, 1H), 1.29 (dt, $J = 8.5, 7.1$ Hz, 6H). ¹³C NMR (75 MHz, CDCl₃) δ 171.2, 168.6, 155.2, 133.3, 119.8, 66.5, 64.3, 61.6, 39.1, 37.3, 34.4, 21.7, 14.4, 14.3 ppm. FT-IR (ATR mode): 3361, 2384, 2938, 1744, 1704, 1657, 1528, 1466, 1447, 1371, 1250, 1142, 1019, 917, 866, 790741, 626 cm⁻¹.

2.4.2. 1-ethyl 1-(2-propionamidoethyl) 2-vinyl cyclopropane-1,1-dicarboxylate [Monomer 2]

1.45 g of 1-(ethoxycarbonyl)-2-vinyl cyclopropane-carboxylic acid (7.9 mmol) was reacted with 1.41 g HOBt-Cl (8.3 mmol), 1.60 g NEt₃ (2.2 mL, 15.8 mmol), 950 mg ethyl (2-aminoethyl)carbamate (7.2 mmol) and 1.63 g DCC (7.9 mmol). DCC was dissolved in 10 mL DCM, added into the reaction mixture, dissolved in 20 mL DCM. Flash chromatography was used for purification (Cyclohexane: EtOAc 100:0 → 8:2). White amorphous solid, yield: 94%. NMR and FTIR experiments were conducted for structural verification (see Figures S12–S18, Supporting Information).

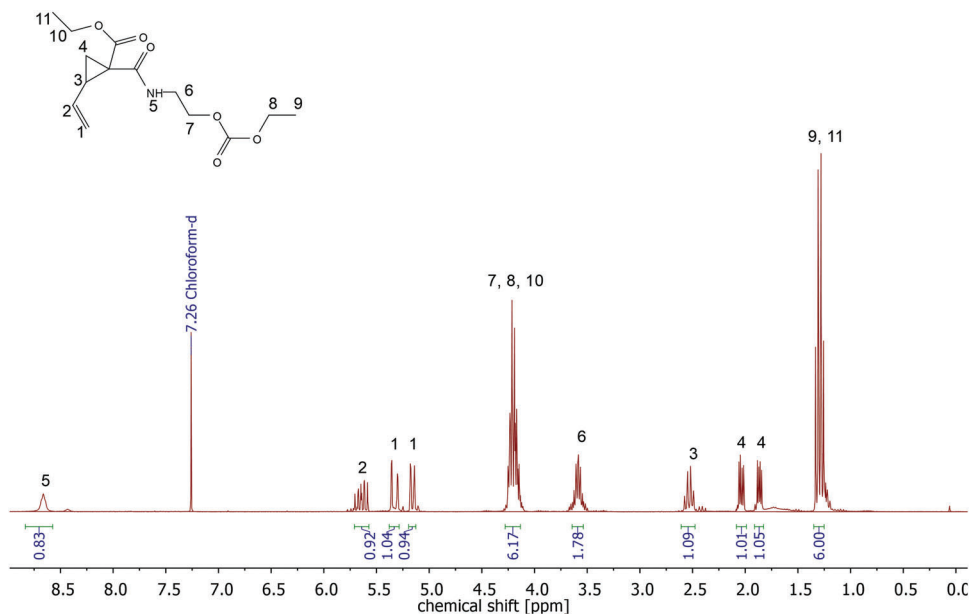


Figure 1. ^1H NMR spectrum of monomer 1 as measured in CDCl_3 .

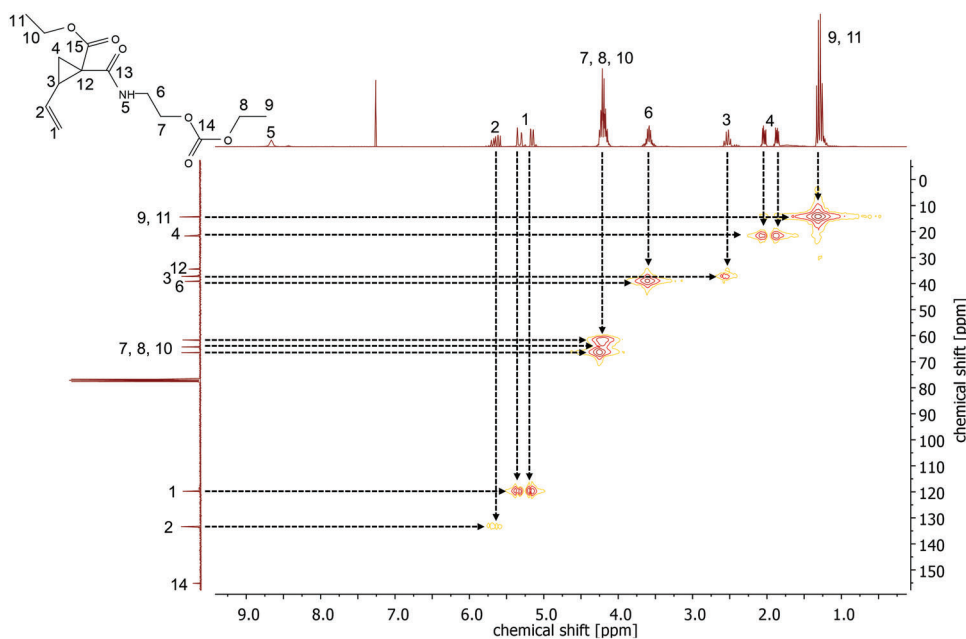


Figure 2. HSQC 2D NMR experiment of monomer 1.

^1H NMR (300 MHz, CDCl_3) δ 8.62 (s, 1H), 5.64 (ddd, $J = 17.1$, 10.2, 8.7 Hz, 1H), 5.37–5.28 (m, 1H), 5.16 (dd, $J = 10.2$, 1.1 Hz, 1H), 4.24–4.04 (m, 4H), 3.49–3.26 (m, 4H), 2.53 (dd, $J = 17.1$, 8.7 Hz, 1H), 2.03 (dt, $J = 8.7$, 4.3 Hz, 1H), 1.87 (dd, $J = 8.0$, 4.3 Hz, 1H), 1.31–1.18 (m, 7H). ^{13}C NMR (75 MHz, CDCl_3) δ 171.3, 169.2, 157.0, 133.3, 119.8, 61.7, 61.0, 41.4, 40.1, 37.2, 34.4, 21.6, 14.8, 14.3 ppm. FT-IR (ATR mode): 3326, 2981, 2929, 1716, 1691, 1641, 1531, 1479, 1450, 1373, 1344, 1314, 1258, 1239, 1146, 1030, 1018, 991, 971, 961, 915, 868, 838, 789, 738, 653 cm^{-1} .

2.4.3. 1-ethyl 1-(2-(3-ethylureido)ethyl) 2-vinyl cyclopropane-1,1-dicarboxylate [Monomer 3]

3.0 g of 1-(ethoxycarbonyl)-2-vinyl cyclopropane-carboxylic acid (16.3 mmol) was reacted with 2.89 g HOBT-Cl (17.0 mmol), 3.30 g NEt_3 (4.5 mL, 32.6 mmol), 1.94 g 1-(2-aminoethyl)-3-ethylurea (14.8 mmol) and 3.36 g DCC (16.3 mmol). DCC was dissolved in 20 mL DCM, added into the reaction mixture, dissolved in 45 mL DCM. Flash chromatography was used for purification (DCM:

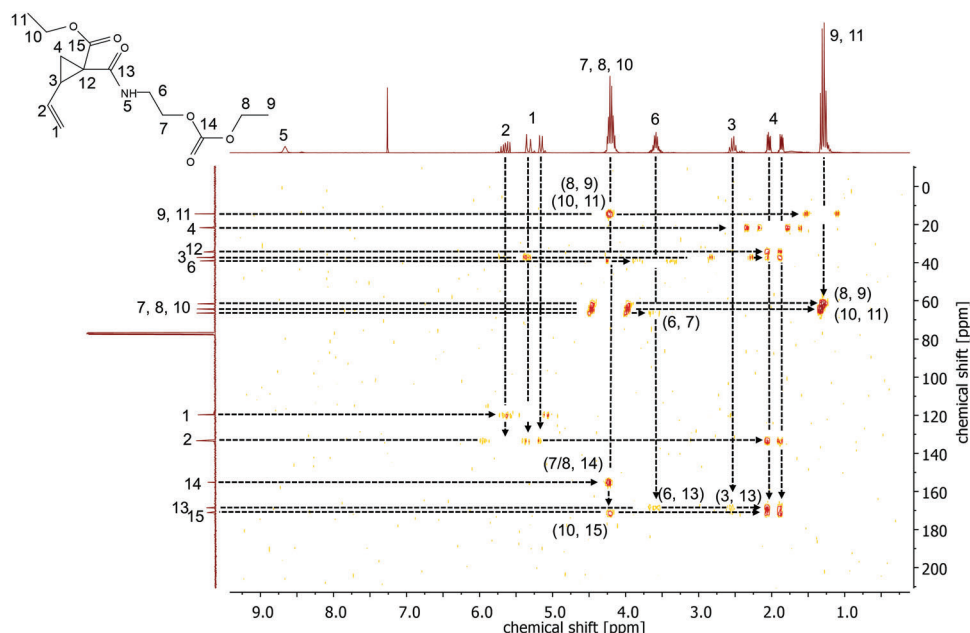


Figure 3. HMBC 2D NMR experiment of monomer 1.

EtOAc 3:7 → 0:100). Light yellow highly viscous liquid, yield: 19%. NMR and FTIR experiments were conducted for structural verification (see Figures S19–S25, Supporting Information).

^1H NMR (300 MHz, CDCl_3) δ 8.69 (s, 1H), 5.75–5.56 (m, 1H), 5.39–5.25 (m, 1H), 5.20–5.09 (m, 1H), 4.29–4.09 (m, 2H), 3.43 (ddt, $J = 10.8, 8.3, 6.0$ Hz, 2H), 3.36–3.26 (m, 2H), 3.18 (q, $J = 7.2$ Hz, 2H), 2.58–2.42 (m, 1H), 2.05–1.93 (m, 1H), 1.93–1.84 (m, 1H), 1.26 (dt, $J = 6.0, 4.8$ Hz, 4H), 1.12 (t, $J = 7.2$ Hz, 3H). ^{13}C NMR (75 MHz, CDCl_3) δ 171.1, 169.7, 158.6, 133.2, 119.8, 61.7, 41.1, 40.5, 37.0, 35.5, 34.5, 21.6, 15.5, 14.3 ppm. FT-IR (ATR mode): 3345, 2978, 2874, 1707, 1633, 1531, 1444, 1372, 1312, 1242, 1142, 1046, 1020, 993, 959, 915, 864, 773, 632 cm^{-1} .

2.4.4. 1-(2-((ethoxycarbonyl)amino)ethyl) 1-ethyl 2-vinyl cyclopropane-1,1-dicarboxylate [Monomer 4]

6.80 g of 1-(ethoxycarbonyl)-2-vinyl cyclopropane-carboxylic acid (36.9 mmol) was reacted with 6.68 g HOBt-Cl (39.4 mmol), 7.64 g NEt_3 (10.5 mL, 75.4 mmol), 3.98 g *N*-(2-aminoethyl) propionamide (34.0 mmol) and 5.47 g DCC (37.7 mmol). DCC was dissolved in 40 mL DCM, added into the reaction mixture, dissolved in 15 mL DCM. Flash chromatography was used for purification (EtOAc: MeOH 100:0 → 9:1). Light yellow viscous liquid, yield: 41%. NMR and FTIR experiments were conducted for structural verification (see Figures S26–S32, Supporting Information).

^1H NMR (300 MHz, CDCl_3) δ 8.73 (s, 1H), 6.38 (s, 1H), 5.64 (ddd, $J = 17.2, 10.1, 8.8$ Hz, 1H), 5.39–5.25 (m, 1H), 5.17 (dd, $J = 10.2, 1.4$ Hz, 1H), 4.19 (q, $J = 7.2$ Hz, 2H), 3.55–3.30 (m, 4H), 2.51 (q, $J = 8.7$ Hz, 1H), 2.20 (q, $J = 7.6$ Hz, 2H), 2.02 (dd, $J = 9.1, 4.3$ Hz, 2H), 1.88 (dd, $J = 8.0, 4.3$ Hz, 1H), 1.28 (t, $J = 7.1$ Hz, 3H), 1.13 (t, $J = 7.6$ Hz, 3H). ^{13}C NMR (75 MHz, CDCl_3) δ 174.5, 171.2, 169.9, 133.2, 119.9, 61.8, 41.0, 39.6, 37.3, 34.3, 29.8, 21.7,

14.3, 10.0. ppm. FT-IR (ATR mode): 3317, 2981, 2939, 1707, 1642, 1529, 1464, 1434, 1372, 1339, 1238, 1143, 1046, 959, 915, 863, 774, 634 cm^{-1} .

2.5. Polymerization

The polymerization was carried out in a glass vial with a septum seal, degassed by purging with argon prior to use. The 5 M monomer solution in anisole was introduced, along with 1 mol% campherquinone (CQ) and 2 mol% ethyl 4-(dimethylamino)benzoate (EDMAB), as a photoinitiator system. The radical light source was a white-light light emitting diode (LED) lamp of GSVITEC Company (Marathon MultiLED). The lamp head consisted of 25 cells. The lamp's power was 800 W halogen equivalents (data as per the lamp manual provided by GSVITEC). The white light LED lamp's emission spectrum was recorded by a Shimadzu fluorescence spectrometer RF type 1502. The white-light LED lamp emits primarily at 442 and 540 nm wavelengths. The light emission between 400 and 480 nm (absorption range of CQ) corresponds to 43% of the lamp head's emitted light's total emission power. The degree of conversion was calculated by gas chromatography (GC). Therefore, to the polymer–monomer mixture, Et_2O for monomers 1 and 4 and toluene for monomers 2 and 3 were added. The solution was stirred for three days, after which the polymer was removed by filtration. The residual monomer was analyzed by GC, using phenol as an internal standard.

3. Results and Discussion

The role of hydrogen bonding in enhancing the polymerization rate and monomer conversion by preorganization of monomers

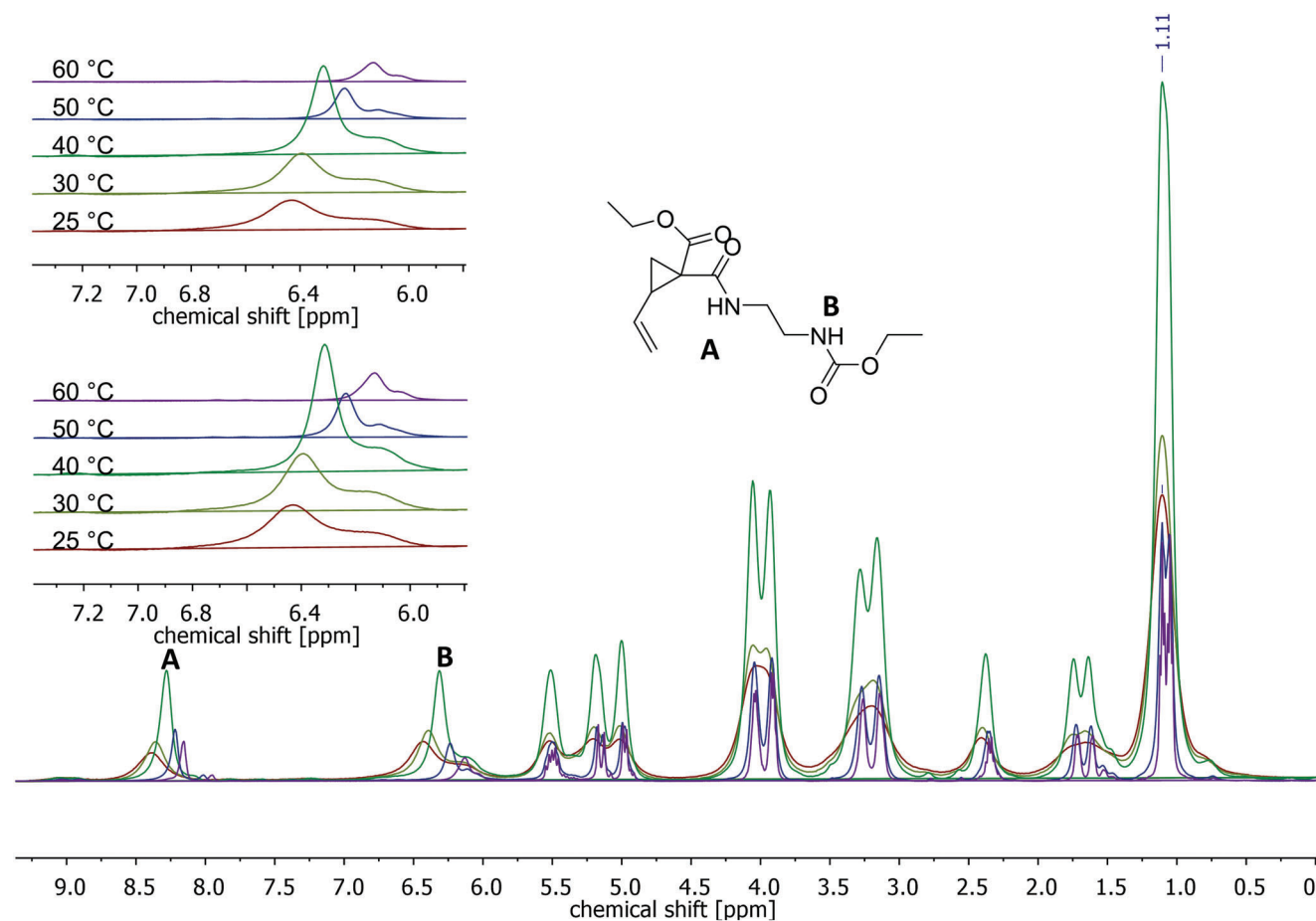


Figure 4. Variable-temperature ^1H -NMR measurements of monomer 2 between 25 and 60 °C.

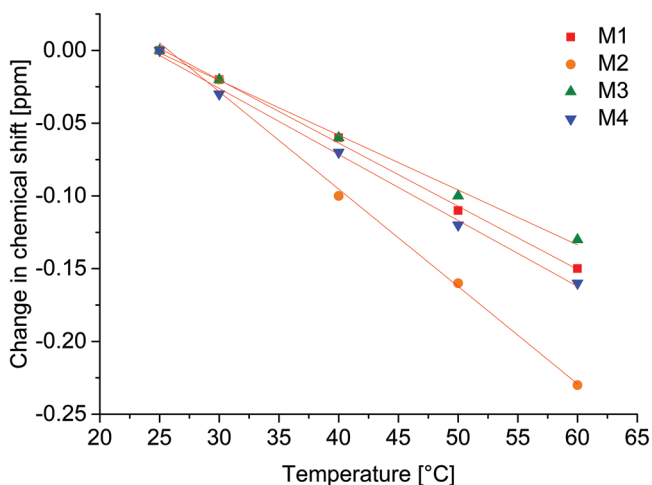


Figure 5. Change of chemical shifts with the temperature of the different NH signals next to the VCP unit of monomers 2–4.

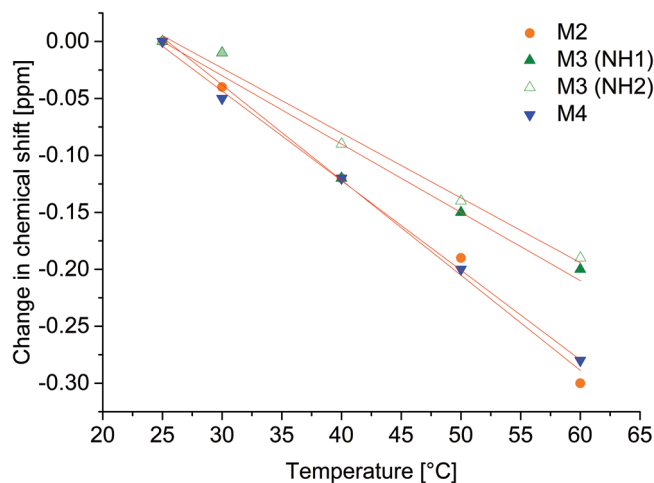


Figure 6. Change of chemical shifts with the temperature of the different NH signals of monomer 2–4 sidechains. The two curves of Monomer 3 belong to the two different urea NH signals.

we showed that hydrogen bonding in the side chain only has a minor effect on the rate of polymerization.^[13] When VCPC(O)NH proton shifts are compared, monomer 2 shows a more signifi-

cant shift than the other three monomers. Monomers 1 and 4 show a comparable shift, while for monomer 3 the change in the chemical shift is the smallest. Monomers 2 and 4 show al-

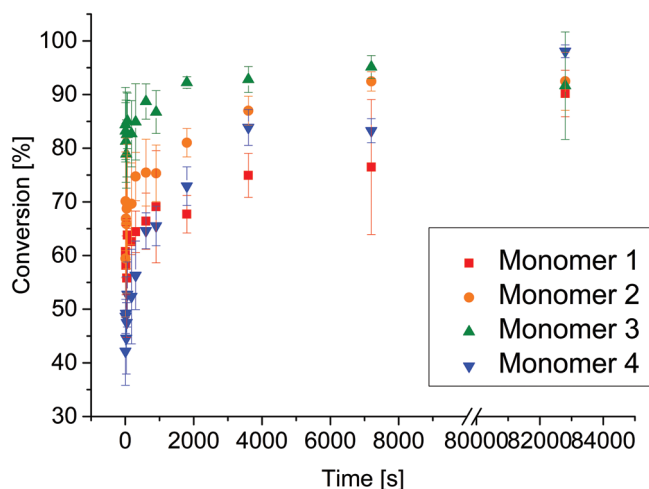


Figure 7. Conversion over time of monomers 1–4. Polymerization was carried out under a LED lamp with a maximum at 440 nm. 1 mol% CQ and 2 mol% EDMAB was used as a photoinitiator.

Table 1. Overall conversion and initial rate (R_p) of photopolymerization of monomers 1–4.

Monomer	R_p [% s ⁻¹]	S_{R_p}	Overall conversion ^{a)} [%]	$S_{conversion}$
1	1.62	0.71	90.2	4.3
2	1.99	0.70	92.5	1.8
3	2.35	0.98	95.1	2.1
4	1.35	0.51	98.7	1.9

Polymerization performed in GSVITEC Company (Marathon MultiLED) Photoreactor, S = standard deviation, ^{a)} by GC measurement (50–300 °C 28 min, internal standard: Phenol).

most the same behavior for the amide protons in the sidechain. For monomer 3 two distinct signals can be observed, both showing a smaller shift. Nevertheless, because of the three hydrogen bond donors, monomer 3 is expected to have the highest degree of preorganization, resulting in the highest rate of polymerization. Monomer 2 shows only two strong hydrogen bonds. Therefore, a slightly lower degree of preorganization can be expected, followed by monomer 4, with two weaker hydrogen bond sites, and monomer 1, with only one hydrogen bond donor.

After this, the free-radical photopolymerizations were followed at different time intervals to study the polymerization rate by following the monomer conversion with time. The monomer conversion versus time plots is given in **Figure 7**. To get a meaningful comparison, the polymerizations were carried out in solvent as the bulk polymerizations were too fast to follow the kinetics by NMR. Also, the physical state of all monomers was not the same (the monomers 1 and 2 were solid whereas 3 and 4 were viscous liquids) making us study polymerization in solution.

The initial rate of polymerization (R_p) was calculated by the average slope of the first three points being 5, 20, and 45 s. The overall conversion is the conversion obtained after 24 h of irradiation. R_p and overall conversion are shown in **Table 1**.

The highest initial R_p with 2.35%/s was observed during the polymerization of monomer 3, followed by monomer 2 (1.99% s⁻¹) and 1 (1.62% s⁻¹). The amide functional group bearing

monomer in the side chain (monomer 4) showed the lowest R_p (1.35% s⁻¹). This trend is maintained for 6 h, when monomer 3 still shows the highest conversion with ≈95%, followed by monomer 2 (≈92%), 4 (≈83%), and 1 (≈76%). Monomer 3 is the fastest polymerizing monomer due to the highest R_p and because it reaches almost complete conversion after 30 min already. There was a slow increase in the conversion after a fast start for other monomers. The H-bonds in urea with two N–H groups are stronger than the N–H/oxygen H-bonds in other functional groups, such as urethane, which is already known in the literature.^[17] This strength might be responsible for the faster polymerization kinetics. One must mention that the strength of hydrogen bonds was calculated from bulk, while the polymerization takes place in solution. For this reason, the solvent effect needs to be considered. The used solvent, anisole, was selected since it does not prevent hydrogen bonding. The ether group can act as a hydrogen bond acceptor^[18] and, therefore, as a bridge between two hydrogen donor-containing monomers.

A comparison between the conversion of the here presented monomers and the corresponding VCPEsters is shown in **Figure S36**, Supporting Information. Although VCPEsters were polymerized in bulk, their polymerization rate is still much slower than that of the corresponding VCP-amides, proving once more the role of preorganization via H-bonding on the rate of polymerization. The only difference between the VCP-Esters and VCP-amides was the linking functional group between the side chain and the VCP ring. It was an H-bond forming –NH group in the case of VCP-amides and –C(O)– group for VCP-esters. Comparison of monomer 1 with the corresponding VCP-esters with the side chain having a carbonate functional group clearly showed the effect of the linking –NH group on the increased rate of polymerization. This effect improves the rate of polymerization and monomer conversions when the sidechain also contains functional groups capable of forming H-bonds.

Monomer 3 and its corresponding VCP-ester with urea functional group in the side chain shows the highest effect of H-bonding depicted in the highest rate of polymerization and the monomer conversions. Interesting to see was almost the exact behavior of VCP-amide and VCP-ester with the amide functional group in the side chain. The synergistic effect of the two H-bonding positions and H-bond strength, in addition to other factors, like a steric hindrance, dipole effects,^[14] and the conformations, might be responsible for this behavior which will be studied in detail in future studies.

The polymers were characterized for molar mass by gel permeation chromatography. The low-medium molar mass polymers were obtained with unimodal GPC curves (**Figure S37**, Supporting Information). To determine the thermal stability, thermal gravimetric analysis (TGA) was performed. While polymer 3 is stable up to 220 °C, changing the urea sidechain to urethane or amide results in an increased onset temperature of 100 K (**Table 2** and **Figure S38**, Supporting Information). With the help of differential scanning calorimetry (DSC), the polymer properties were investigated (for curves, see **Figure S39**, Supporting Information). No melting peak is observed in the shown temperature range, leading to amorphous polymers. Polymer 1 has a T_g at 32 °C, around room temperature, while the T_g increases from polymer 2 (55 °C) over polymer 4 (69 °C) toward polymer 3 (89 °C). The low T_g of polymer 1 can be explained by the side

Table 2. Properties of polymers 1–4, containing glass transition temperature, degradation temperature, molecular weight, and weight distribution.

Polymer	$\overline{M}_n^a)$	D_M	T_g [°C] ^{b)}	T_{onset} [°C] ^{c)}
1	$6.9 \cdot 10^3$	2.10	32	275
2	$1.6 \cdot 10^4$	2.14	55	324
3	$1.1 \cdot 10^4$	1.34	89	221
4	$4.6 \cdot 10^4$	–	69	323

^{a)} GPC (DMF, PS standard); ^{b)} DSC (-60 – 150 °C, N₂, 20 K min⁻¹, T_{onset}); ^{c)} TGA (25–600 °C, N₂, 10 K min⁻¹).

chain, where no hydrogen bond can be formed. This way, flexibility between polymer chains is increased. While the difference between polymers 2 and 4 might be due to the difference in molecular weight, the high T_g of monomer 3 is explained by the higher degree of preorganization from the urea side chain.

3.1. Theoretical Calculations

We carried out molecular dynamics (MD) simulations using GROMACS software for the theoretical part. The structure and topology for the four VCP amide derivatives were created using automated topology builder (ATB) site,^[19] and the GROMOS54a7 all-atom force field^[20] was used throughout all the simulations. The automated topology builder (ATB) handles the issue of creating force-fields models for molecules not known or studied previously, thereby allowing the user to extract GROMOS-compatible topologies for virtually any molecule. All the parameters (bonded and non-bonded) were kept as provided in the original ATB topology files. They can be tracked by inserting the IUPAC InChI key provided in the Supporting Information into the ATB database. The foundational form of the atomistic force field in this work follows the equation below. For short-range forces, we apply a harmonic potential for bond stretching and angle bending and a dihedral potential for torsion. For long-range forces, we use Coulomb force for electrostatic interactions and Lennard Jones 12_6 (LJ 12_6) for van der Waals interactions.

$$\begin{aligned}
 V = & \sum_{\text{bonds}} \frac{1}{2} k_{\text{bonds}} (r - r_0)^2 + \sum_{\text{angles}} \frac{1}{2} k_{\text{angle}} (\theta - \theta_0)^2 \\
 & + \sum_{\text{torsions}} \frac{1}{2} k_{\phi} (1 + \cos(n\phi - \phi_s))^2 + \sum_{\text{Coulomb}}^{i < j} \frac{q_i q_j}{r_{ij}} \\
 & + \sum_{\text{vdW}}^{i < j} \left\{ 4\epsilon_{ij} \left[\left(\frac{\sigma_{ij}}{r_{ij}} \right)^{12} - \left(\frac{\sigma_{ij}}{r_{ij}} \right)^6 \right] \right\} \quad (1)
 \end{aligned}$$

Four simulation boxes of initial dimensions $7 \times 7 \times 7$ nm³ with periodic boundary conditions in all dimensions were filled with one type of monomer each. The number of monomers was 404, 397, 390, and 416 for types 1, 2, 3, and 4. NPT simulations were carried out at 300 K for 125 ns with 1 fs time step. The box size shrunk because of the NPT ensemble to give average side lengths of 5.50533, 5.53847, 5.55004, and 5.55921 nm for monomers 1, 2, 3, and 4, respectively.

The Verlet neighbor search^[21] scheme was used to update the neighbor list, whereas short-range electrostatic, as well as van der Waals cutoff, was set to 1.0 nm, and particle mesh ewald (PME)^[22] with cubic interpolation for long-range electrostatics was used. Parrinello-Rahman barostat^[23] and velocity rescaling thermostat^[24] were applied to maintain a constant pressure of 1 bar and temperature at 300 K, respectively. Hydrogen bonds were constrained using the LINCS algorithm.^[25] A snapshot of the simulation box filled with monomer 1 is shown in **Figure 8a**. **Figure 8b–e** present the individual atomistic structures used for monomers 1, 2, 3, and 4 respectively.

Of the total 125 ns simulations, the last 115 ns were used for RDF and H-bond calculations. The root mean squared deviation (RMSD) curves reach a plateau after the first 10 ns implying that the system has reached equilibration (documented in the SI). The resulting trajectories were analyzed using the Gromacs tools *gmx hbond*, *gmx rdf*, and *gmx rms*. The hydrogen bonds were derived based on the distance cutoff of 0.35 nm between the hydrogen and the acceptor and an angle cutoff of 30° for the hydrogen – donor-acceptor angle. They are shown in **Figure 9a** as a function of time. The OH and NH groups were considered donors and O and N as acceptors. The average number of H-bonds in monomers 1, 2, 3, and 4 are 285, 323, 528, and 334, respectively and are shown in **Figure 9b** with error calculation.

To examine if there exists pre-existing order due to hydrogen bonding, we calculate the angle one monomer's C=C makes with the other and compute Herman's orientation parameter^[26] or S-factor

$$S = \langle P_2 \cos \theta \rangle = \frac{3 \langle \cos^2 \theta \rangle - 1}{2}$$

The value of the above equation in case of perfect alignment is $S = 1$, in case of partial alignment is $0 < S < 1$, for a completely random alignment is $S = 0$ and for an anti-aligned system is $S = 0.5$. **Figure 10a** presents the S factor as a function of time, and **Figure 10b** shows its average with error bars (calculated via block averaging). As seen from **Figure 10a,b**, all monomers have their S factor ≈ 0.25 . The values are close to zero, indicating that the monomers are almost randomly arranged. They all have an S factor in the same range, which shows no difference in arrangement preference before polymerization for all the four monomers.

Furthermore, **Figure 11a** shows the radial distribution functions (RDF) for the first in the C=C bond (termed C1, see Supporting Information) and **Figure 11b** for the carbon atom next to the functional group of the side chain (termed C10, see Supporting Information) for all the four monomers. The RDFs show no difference for the first carbon atoms in **Figure 11a**, indicating no difference in the distance distribution for all monomers near the cyclic region. The RDFs of the carbon atom of the side chain (C10) shown in **Figure 11b** also show a similar trend. Thus, all the monomers are similarly aligning themselves before polymerization.

The time behavior of other properties, such as root-mean-square deviation, time convergence of simulations, and the radial distribution functions between individual atoms, are provided in the Supporting Information.

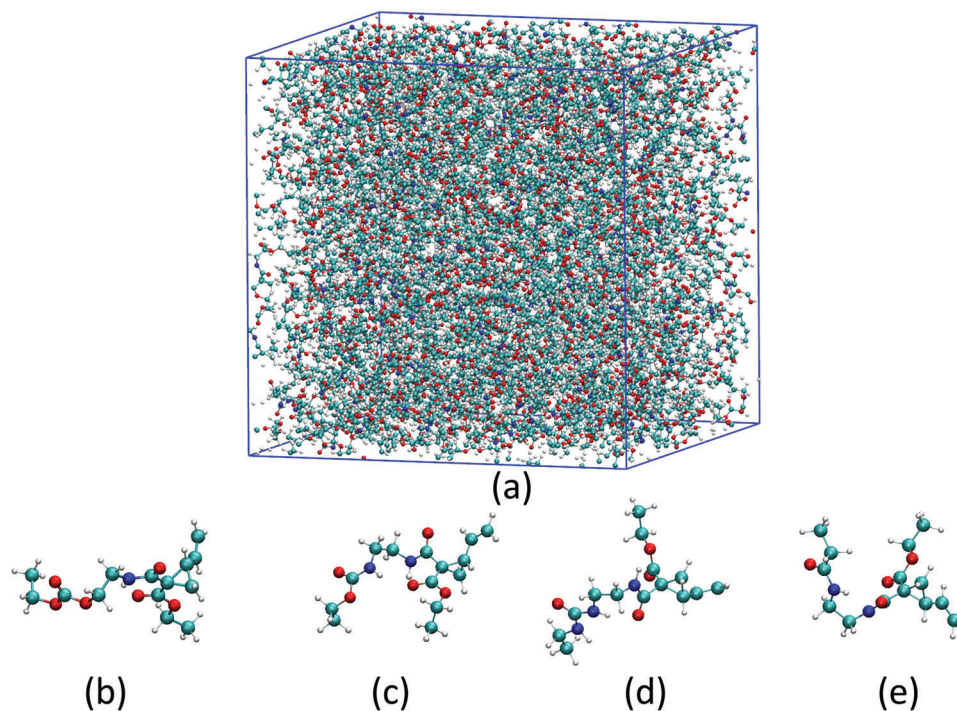


Figure 8. a) Snapshot of the simulation box in the NPT ensemble. Structures of b) monomer 1, c) monomer 2, d) monomer 3, and e) monomer 4, used during simulations.

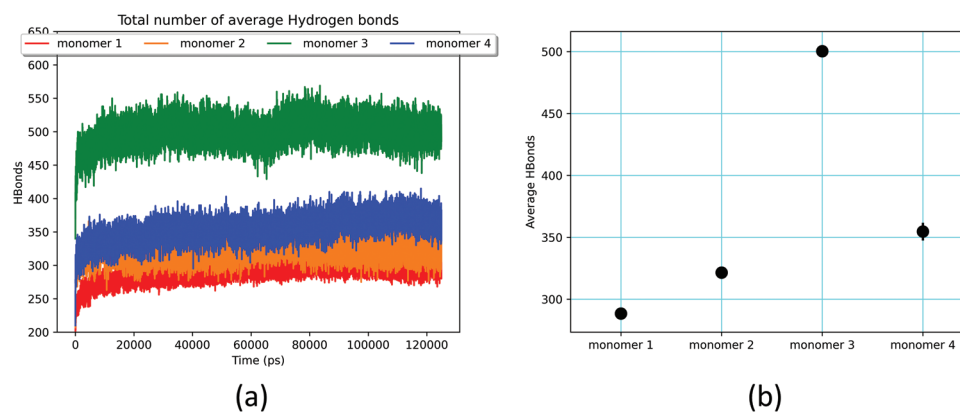


Figure 9. a) The average number of H-bonds of the system as a function of time. b) The total number of H-bonds averaged over time.

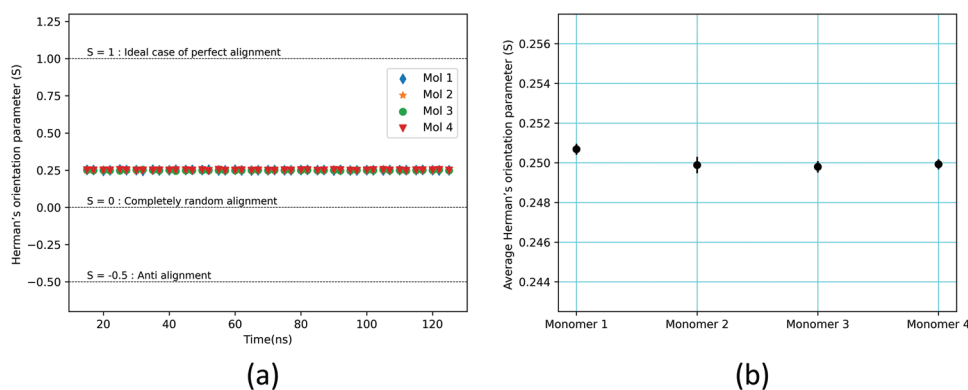


Figure 10. S factor calculated for angles between double C=C for all the averaged over all the monomers as a) a function of time and b) averaged over time.

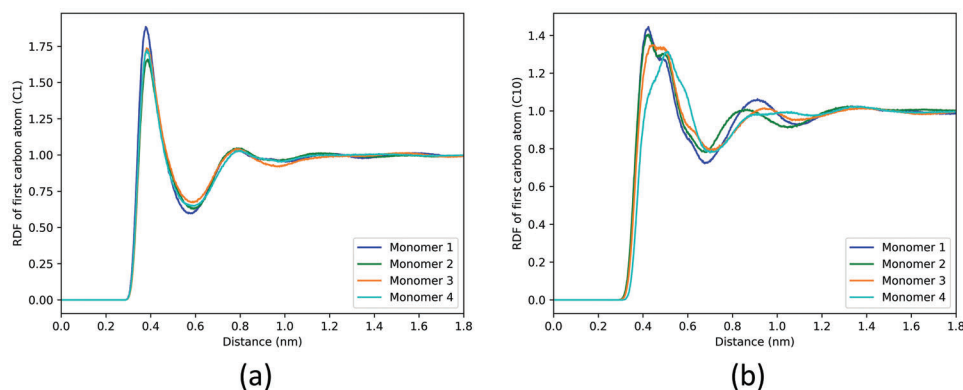


Figure 11. Radial distribution function for a) the first and b) the last carbon atoms of the monomers

4. Conclusions

Four new monofunctional VCPs, containing an amide linkage to their side chains have been synthesized. The number and strength of hydrogen bonds have been investigated. The urea containing monomer 3, with the highest amount of possible hydrogen bonds, showed the highest rate of polymerization and overall conversion. Monomer 2 (urethane) shows a stronger hydrogen bonding compared to monomer 1 + 4 and also a higher rate of polymerization. While the amide containing monomer 4 can form two hydrogen bonds, the strength of the VCPC(O)NH donor in comparison to monomer 1 (carbonate) is the same. A similar rate of polymerization suggests the high dependency between the hydrogen bond and polymerization speed. In general, the amide-linked VCPs showed a much faster polymerization than the ester-linked ones investigated in our previous work.^[15] Theoretical calculations showed only a slight difference in the number of hydrogen bonds between monomers 1, 2, and 4, suggesting that the side chain does not form many bonds in their case. For monomer 3, almost twice the amount of hydrogen bonds could be observed. All monomers show a similar alignment and energy pattern, suggesting that hydrogen bonds do not play any role in the orientation of the monomers but have a massive role in their polymerization speed. This knowledge helps selectively design new bifunctional fast polymerizable VCPs with a complete conversion.

Supporting Information

Supporting Information is available from the Wiley Online Library or from the author.

Acknowledgements

The authors sincerely thank Prof. J. Senker (ACIII) from the University of Bayreuth for the solid-state NMR measurements. S.A. and S.S. thank DFG for the financial support. S.G. and S.P. thank the Volkswagen Foundation for financial support.

Open access funding enabled and organized by Projekt DEAL.

Conflict of Interest

The authors declare no conflict of interest.

Author Contributions

S.S. carried out all experimental work. S.P. made theoretical calculations. S.A. created, designed, and supervised the project. S.G. supervised the theoretical part. The manuscript was written with the contributions of all authors. All authors have approved the final version of the manuscript.

Data Availability Statement

The data that support the findings of this study are available in the supplementary material of this article.

Keywords

hydrogen bonding, photopolymerization, preorganization, theoretical calculation, vinyl cyclopropane

Received: May 12, 2022
Revised: July 6, 2022
Published online: August 2, 2022

- [1] a) J. Wang, S. A. Blaszczyk, X. Li, W. Tang, *Chem. Rev.* **2021**, *121*, 110; b) A. Delbrassinne, M. Richald, J. Janssens, R. Robiette, *Eur. J. Org. Chem.* **2021**, *2021*, 2862; c) T. Hudlicky, *ACS Omega* **2018**, *3*, 17326.
- [2] a) D. H. Seuyep, N. G. A. Luinstra, P. Theato, *Polym. Chem.* **2013**, *4*, 2724; b) J. Zhou, L. Fang, J. Wang, J. Sun, K. Jin, Q. Fang, *Polym. Chem.* **2016**, *7*, 4313; c) D.-F. Chen, B. M. Boyle, B. G. McCarthy, C.-H. Lim, G. M. Miyake, *J. Am. Chem. Soc.* **2019**, *141*, 13268.
- [3] a) D.-F. Chen, S. Bernsten, G. M. Miyake, *Macromolecules* **2020**, *53*, 8352; b) N. Moszner, T. Völkel, F. Zeuner, V. Rheinberger, *Macromol. Symp.* **2000**, *153*, 151.
- [4] P. P. Contreras, P. Tyagi, S. Agarwal, *Polym. Chem.* **2015**, *6*, 2297.
- [5] Y. Catel, U. Fischer, P. Fässler, N. Moszner, *Macromol. Chem. Phys.* **2016**, *217*, 2686.
- [6] F. Sanda, T. Takata, T. Endo, *Macromolecules* **1993**, *26*, 1818.
- [7] Y. Jian, Y. He, L. Zhao, A. Kowalczyk, W. Yang, J. Nie, *Adv. Polym. Technol.* **2013**, *32*, 21331.
- [8] N. Moszner, F. Zeuner, T. Völkel, V. Rheinberger, *Macromol. Chem. Phys.* **1999**, *200*, 2173.
- [9] C. Decker, *Macromol. Rapid Commun.* **2002**, *23*, 1067.
- [10] F. Sanda, T. Takata, T. Endo, *Macromolecules* **1994**, *27*, 3982.
- [11] P. Pineda Contreras, C. Kuttner, A. Fery, U. Stahlschmidt, V. Jérôme, R. Freitag, S. Agarwal, *Chem. Commun.* **2015**, *51*, 11899.

- [12] a) H. Chiba, K. Kitazume, S. Yamada, T. Endo, *J. Polym. Sci. Part A: Polym. Chem.* **2016**, *54*, 39; b) Y. Catel, P. Fässler, U. Fischer, C. Gorsche, R. Liska, S. Schörpf, S. Tauscher, N. Moszner, *Eur. Polym. J.* **2018**, *98*, 439; c) N. Takahashi, A. Sudo, T. Endo, *Macromolecules* **2017**, *50*, 5679; d) P. Pineda Contreras, *Dissertation*, Bayreuth, **2017**.
- [13] S. Schumacher, S. Pantawane, S. Gekle, S. Agarwal, *Macromolecules* **2021**, *54*, 11.
- [14] J. F. G. A. Jansen, A. A. Dias, M. Dorschu, B. Coussens, *Macromolecules* **2003**, *36*, 3861.
- [15] V. Alupei, H. Ritter, *Macromol. Rapid Commun.* **2001**, *22*, 1349.
- [16] a) B. Attenni, M. Donghi, C. Gardelli, M. Meppen, F. Narjes, B. Pacini, WO 2008/142055 A2, **2008**; b) K. Ito, Y. Uesaka, T. Akiike, CN 106479519 A, **2016**; c) H. Solařová, I. Císařová, P. Štěpnička, *Organometallics* **2014**, *33*, 4131; d) T. Fang, C. Sun, Y. Xu, J. Yuan, Y. Wang, J. Xing, *Chem. Res. Chin. Univ.* **2014**, *30*, 931.
- [17] J. Mattia, P. Painter, *Macromolecules* **2007**, *40*, 1546.
- [18] J. P. M. Lommerse, S. L. Price, R. Taylor, *J. Comput. Chem.* **1997**, *18*, 757.
- [19] A. K. Malde, L. e Zuo, M. Breeze, M. Stroet, D. Poger, P. C. Nair, C. Oostenbrink, A. E. Mark, *J. Chem. Theory Comput.* **2011**, *7*, 4026.
- [20] N. Schmid, A. P. Eichenberger, A. Choutko, S. Riniker, M. Winger, A. E. Mark, W. F. van Gunsteren, *Eur. Biophys. J.* **2011**, *40*, 843.
- [21] L. Verlet, *Phys. Rev.* **1967**, *159*, 98.
- [22] T. Darden, D. York, L. Pedersen, *J. Chem. Phys.* **1993**, *98*, 10089.
- [23] M. Parrinello, A. Rahman, *J. Appl. Phys.* **1981**, *52*, 7182.
- [24] G. Bussi, D. Donadio, M. Parrinello, *J. Chem. Phys.* **2007**, *126*, 14101.
- [25] B. Hess, H. Bekker, H. J. C. Berendsen, J. G. E. M. Fraaije, *J. Comput. Chem.* **1997**, *18*, 1463.
- [26] a) G. R. Mitchell, A. Tojeira, *Controlling the Morphology of Polymers. Multiple Scales of Structure and Processing*, Springer International Publishing, Cham **2016**; b) Orientation order parameter, http://gisaxs.com/index.php/Orientation_order_parameter (accessed: August 2020)